A Pragmatic Approach for Lens Distortion Correction from a Fictitious Image

Naa Dedei Tagoe[1], Heinz Rüther[2], Julian Smit[3]

[1,2,3]Geomatics Division, University of Cape Town, Cape Town, South Africa,
[1]tgxnaa001@myuct.ac.za, [2] Heinz.ruther@uct.ac.za [2] Julian.smit@uct.ac.za

This paper has been through a process of double-blind peer review

Abstract

The paper offers a pragmatic alternative to the mathematical modelling of lens distortion. The method was developed as a proof of concept for application in the photogrammetric restitution of objects and buildings from photographic panoramas. The method quantifies the distortion characteristics of a lens-camera combination by comparing near distortion-free fictitious image coordinates with real (distorted) image coordinates. Based on the differences between fictitious and real image coordinates, a distortion matrix, equivalent to a look-up table, is created which describes the distortion characteristics of the camera-lens combination. The distorted images are subsequently rectified using a backward pixel mapping strategy.

As a check of the effectiveness of the proposed technique, a best-fit line function is used to verify that a straight line in object space appears as straight line on the image after rectification. The standard deviations before (180.6µm equivalent to 28 pixels) and after (17.5µm or approximately 3 pixel) fitting the best-fit line indicate that the lens distortion has been minimised.

To further characterise the performance of the proposed method, a subset of the control points was used to form the distortion matrix. The known locations of the remaining randomly selected control points were compared with their interpolated values. It was observed that the denser the control points the more precise the interpolated values indicating that the proposed method is dependent on the distribution and density of control points.

1. Introduction

Panoramas are an important component of the Zamani database (Rüther, 2002; Rüther, 2011; Rüther *et al.*, 2012), with their use presently being restricted to visualization of sites.

G. Fangi proposed the idea of Spherical Photogrammetry in 2007 and extended the photogrammetric bundle theory to panoramic images (Fangi, 2007). Though a powerful photogrammetric tool for the documentation and survey of the heritage structures, orientation and restitution procedures are still manual (Fangi, 2007; Fangi, 2010; Fangi *et al.*, 2013). Currently, no commercial software package exists for the 3D reconstruction from spherical panoramas.

In the course of the research within the Zamani Project, the use of spherical panoramas as proposed by Fangi as an additional tool for the creation of 3D models of heritage structures is being

explored. As the panoramas acquired for the Zamani project are largely captured with fisheye lenses, an image rectification approach had to be developed specifically for this purpose.

Traditional photogrammetric lens distortion models have proved efficient for classical lenses (conventional and most wide-angle lenses). However, they failed when applied to fisheye lenses because classical lenses are based on central perspective projection while fisheye lenses are based on other projection models such as stereographic, equidistance and equisolid angle projection resulting in high levels of distortion (Kannala and Brandt, 2006; Hughes *et al.*, 2010). In this paper, a proof of concept for a pragmatic image rectification approach from fictitious image is proposed.

2. Lens Distortion Modelling for Photogrammetric Applications

The concept of bundle adjustment was originally developed for Analytical Photogrammetry, where it is the most widely used algorithm for photogrammetric restitution and 3D point determination. The method was first developed by D.C. Brown (1956; 1964; 1976) and H. H. Schmid (1956) and has since undergone numerous improvements and additions.

Departures from the collinearity condition, on which the photogrammetric bundle theory is based, result in systematic errors. To reduce the effect of these errors, the bundle adjustment equation is usually extended by a set of additional parameters (APs) (Brown, 1971; Fraser, 1997). The number of APs in the various models developed over time varies widely and models with up to 50 parameters have been proposed in which cases there is a danger of over-parameterization (Fraser, 1982). The systematic errors typically associated with digital cameras include symmetric radial distortion, decentering distortion, image plane unflatness (bowing of image chips) and in-plane image distortion.

Radial lens distortion is caused by imperfect lens construction which leads to failure in the transmission of straight lines. This distortion causes image points to be displaced radially from their ideal position towards or away from the image centre. Decentering lens distortion is caused by the misalignment of the elements of the lens system. This causes both radial and tangential displacement. In-plane image distortion, originally introduced to account for affine distortions of film, also plays a role in the calibration of digital cameras where electronic effects can cause similar phenomena, however, they are generally insignificant and often ignored. Deviations from the flatness of the image plane may be introduced as a result of imperfection during manufacturing or aging. The amount of image point displacement due to image plane unflatness is a function of the deviation of the image plane from flatness and the incidence angle of the imaging ray. Because of this, the effect of image plane unflatness is more significant in wide-angle lenses with short focal lengths compared to narrow-angle lenses with long focal lengths (Fraser, 1997). A literature search did not reveal photogrammetric approaches to the modelling of image plane unflatness, other than early réseau-based methods (Sadler, 1958; Robinson, 1963; Ziemann, 1968). However, direct

physical measurements of the imaging chip surface were employed to correct the lack of flatness.

The net image distortion at any point on the image is given by Equation 1 (Fraser *et al.*, 1995; Fraser, 1997):

$$\Delta x = \Delta x_{\mathbf{r}} + \Delta x_{d} + \Delta x_{\mathbf{u}} + \Delta x_{\mathbf{f}}$$

$$\Delta y = \Delta y_{r} + \Delta y_{\mathbf{d}} + \Delta y_{u} + \Delta y_{f} \qquad [1]$$

where the subscript r is for radial distortion, d is for decentering distortion, u is for image plane unflatness and f is for in-plane image distortion.

3. Conventional Photogrammetric Lens Distortion Model

An account of the evolution of lens distortion modelling and correction is provided in Clarke and Fryer (1998). The most widely used lens distortion model adopted by the photogrammetric community was proposed by D. C. Brown and dates back to the era of Analytical Photogrammetry. In 1966, Brown published a paper - "De-centering Lens Distortion" - which was based on an earlier paper he presented at the 1965 Annual Convention of American Photogrammetric Society, which addressed decentering lens distortion in metric cameras by reconciling two earlier conflicting theories: Thin prism theory and Conrady's model. In 1971, Brown classified lens distortion as radial and decentering distortion and suggested a corresponding algorithm to determine lens distortion parameters. Based on an original formulation by Magill (1955), Brown (1971) derived an 8-parameter lens distortion formula (Equation 2) for the correction of image coordinates (x', y'):

$$x' = x + \hat{x}(K_1 r^2 + K_2 r^4 + K_3 r^6 + \cdots) + [P_1(r^2 + 2\hat{x}^2) + 2P_2\hat{x}\hat{y}][1 + P_3 r^2 + \cdots]$$

$$y' = y + \hat{y}(K_1 r^2 + K_2 r^4 + K_3 r^6 + \cdots) + [2P_1\hat{x}\hat{y} + P_2(r^2 + 2\hat{y}^2)][1 + P_3 r^2 + \cdots] \qquad [2]$$

in which;

$$\hat{x} = x - x_o$$
$$\hat{y} = y - y_o$$
$$r = [(x - x_o)^2 + (y - y_o)^2]^{1/2}$$
$$x' - x = \Delta x$$
$$y' - y = \Delta y$$

where (x, y) and (x', y') are the observed and corrected image coordinates, (Δx, Δy) are the correction for observed image coordinates, x_p, y_p the principal point offsets, K_1, K_2, K_3 the coefficients of radial distortion and P_1, and P_2 the coefficients of decentring distortion. The high order parameter P_3 for the decentering component is often ignored.

In Fraser *et al.* (1995) and Fraser (1997), a 10-parameter lens distortion model was proposed.

The model is similar to Brown's 'standard' 8-parameter model supplemented with two terms to account for first-order in-plane image distortion. Additionally, Fraser's model ignores P_3 and includes the camera constant (c) as a parameter.

$$\Delta x = x_o - \frac{\hat{x}}{c}\Delta c + \hat{x}r^2K_1 + \hat{x}r^4K_2 + \hat{x}r^6K_3 + (2\hat{x}^2 + r^2)P_1 + 2P_2\widehat{xy} + b_1\hat{x} + b_2\hat{y}$$

$$\Delta y = y_o - \frac{\hat{y}}{c}\Delta c + \hat{y}r^2K_1 + \hat{y}r^4K_2 + \hat{y}r^6K_3 + 2P_1\widehat{xy} + (2\hat{y}^2 + r^2)P_2 \quad [3]$$

where (x, y) and (x', y') are the observed and corrected image coordinates, (Δx, Δy) are the correction for observed image coordinates Δc represents a correction to the initial principal distance value and b_1 and b_2 are in-plane correction parameters to model shear. For digital cameras, in-plane image distortion is not significant and the values for $b_1$and b_2 can be ignored (Fraser *et al.*, 1995; Fraser, 1997).

While the above models have proved efficient for the correction of lens distortion for classical lenses, they failed when applied to fisheye lenses mainly because the classical and fisheye lenses are based on different projection models.

4. A Lens Distortion Correction Technique using Fictitious Image Coordinates

This paper proposes the determination of numerical lens distortion characteristics for fisheye lenses through the comparison of a near-error-free simulated image point positions of targets of a testfield with the real image of these targets. This approach is a pragmatic, assumption-free alternative to early methods (Basu and Licardie, 1995; Kannala and Brandt, 2004; Kannala and Brandt, 2006; Kedzierski and Fryskowska, 2008; Schneider *et al.*, 2009; Hughes *et al.*, 2010; Arfaoui and Thibault, 2013) proposed for the rectification of fisheye lenses which is based on a theoretical model.

The testfield used for this purpose is a planar point array of 91 calibration points with known xyz positions located in the Geomatics Division at the University of Cape Town. The points are well distributed over an area of approximately 6m by 2.5m and represented by circular targets in the form of white retro-reflective disks of 14mm diameter on black background (Figure 1). The three-dimensional (3D) positions of these targets were determined with sub-millimetre accuracy by means of theodolite measurements (horizontal and vertical angles) from a three-point base line.

The procedure for determination of numerical lens distortion characteristics include:

a) Preliminary camera calibration and fictitious image generation
b) Determination of numerical lens distortion characteristics by comparison of actual and error

free virtual images

c) Image rectification using fictitious image coordinates

Figure 1. Testfield at University of Cape Town

4.1 Preliminary camera calibration and fictitious image generation

In order to obtain approximation values for the camera constant, principal point position and the exterior orientation parameters, as required for the generation of a fictitious image (Rüther, 1982); a standard camera calibration is carried out. Fifteen (15) images of the testfield are taken from various camera stations ensuring good ray intersection and roll diversity.

The fictitious image is created to be distortion-free; hence the image coordinates are based on the non-linear collinearity equation without APs (Equation 4):

$$x' = x_p - c\frac{r_{11}(X_i - X_c) + r_{12}(Y_i - Y_c) + r_{13}(Z_i - Z_c)}{r_{31}(X_i - X_c) + r_{32}(Y_i - Y_c) + r_{33}(Z_i - Z_c)}$$

$$y' = y_p - c\frac{r_{21}(X_i - X_c) + r_{22}(Y_i - Y_c) + r_{33}(Z_i - Z_c)}{r_{31}(X_i - X_c) + r_{32}(Y_i - Y_c) + r_{33}(Z_i - Z_c)} \quad [4]$$

where;

$x', y' =$ fictitious image coordinates of a point

$x_p, y_p =$ principal point coordinates

$X_i, Y_i, Z_i =$ object space coordinate of a point

$X_c, Y_c, Z_c =$ approximate camera position

$c =$ camera constant

The values for the elements of interior and exterior camera orientation applied in the fictitious image generation process are only approximations derived from bundle adjustment without

distortion corrections. The method proposed here derives the distortion characteristics of a camera-lens combination from a single image out of a multi-image array. The position of this image is chosen to be central to the planar calibration field (in red-blue as shown in Figure 2). While the central image is used to establish the image distortions, the entire image array is employed in a multi-image bundle adjustment approach using Australis software to determine the initial exterior orientation parameters for this image. The alternative of a single image space resections was considered to be of inferior accuracy in this regard and the bundle adjustment was adopted as a more stable solution. An additional problem arose as a result of the typically large distortions at the outer image areas of a fisheye image. To reduce this detrimental effect on the determination of the exterior camera parameters, only points in the central image areas were used for the bundle solution. The portion of the image, acceptable for this step should be established empirically in each case. The accuracy of the entire process can be improved by iteration.

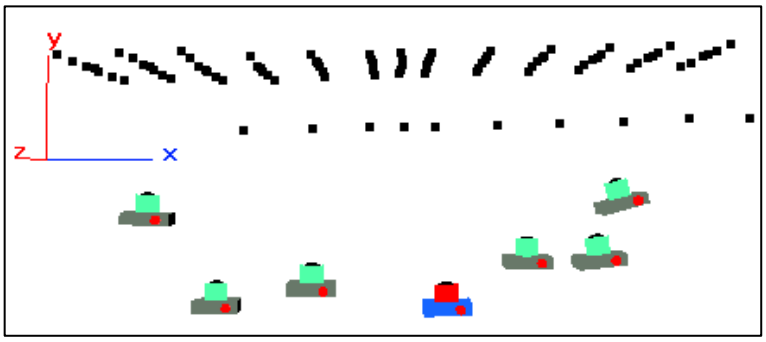

Figure 2. Plan view of calibration field showing central image

4.2 Determination of numerical lens distortion characteristics

The distortion characteristics of the lens are then quantified by determining differences (Δx, Δy) between the fictitious, distortion-free (x', y') and real, distorted (x, y) image coordinates. Distortion amounts for specific positions on the camera's sensor/chip where the targets were imaged. This can be expressed as Equation 5:

$$\begin{bmatrix}\Delta x_i\\ \Delta y_i\end{bmatrix}_{1,2n} = \begin{bmatrix}x_i'\\ y_i'\end{bmatrix}_{1,2n} - \begin{bmatrix}x_i\\ y_i\end{bmatrix}_{1,2n} \quad [5]$$

where:

$x', y' = \text{distortion} - \text{free fictitious image coordinates}$

$x, y = \text{measured coordinates of the real image}$

$\Delta x_i, \Delta y_i = \text{departures from collinearity (distortion amounts in x and y)}$

$n = \text{number of control points}$

$i = \text{control point's id}$

In the next step, a distortion matrix or look-up table is created in which each pixel in a

calibration image is allocated a distortion value derived by interpolating between the calibration points using a biharmonic surface fitting model. Distortion values for pixels at the edges of the calibration image (outside the imaged calibration targets) have to be extrapolated, which suggests that attempts have to be made to capture image in such a way that target points appear close to the edge of the images.

4.3 Image Rectification from fictitious image coordinates

In a final step, the position of the distorted pixel is corrected to its undistorted position using a backward pixel mapping strategy. Backward mapping was chosen over forward mapping to avoid the creation of multiple values for a pixel in the resulting undistorted image. These mapping processes are similar to those used for digital ortho-image generation.

The procedure involves taking a pixel location on the corrected but still blank image as input (Figure 3) and determining which original pixel on the distorted image maps to this location after application of the distortion correction values (Δx, Δy) from the calibration image or matrix. RGB values are then extracted from the distorted image. As these image positions are floating point values and do not correspond to integer pixels, their RGB values are interpolated from the RGB values of surrounding pixels. Although bicubic interpolation is a suitable option as it involves a reduced loss in contrast and a reduction of the lowpass filtering effect, bilinear interpolation was chosen in this investigation of the analytical method because of its computational advantages over bicubic interpolation.

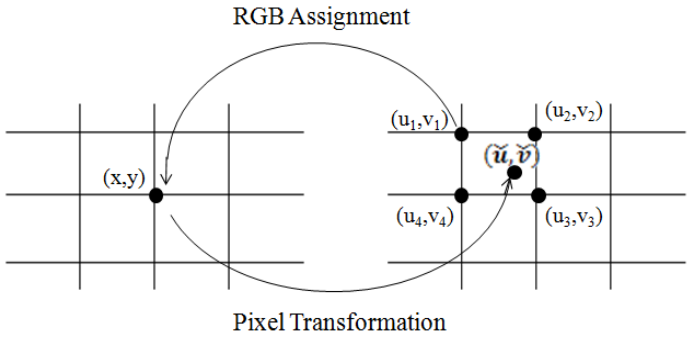

(a)Undistorted Image (b) Distorted Image

Figure 3. Backward pixel mapping method

5. Experimental Results and Analysis

Preliminary experiment on the image rectification process was carried out using the fifteen (15) images of the testfield. The images were acquired with Nikon D200, AF Fisheye 10.5mm Nikkor lens with sensor and pixel sizes of 3872 x 2592 (pixels) and 6.4µm respectively. Figures 4a and 4b show an example of the images of the testfield before and after rectification respectively. As can be observed, the barrel effect in Figure 4a has been removed through the rectification process (Figure

4b).

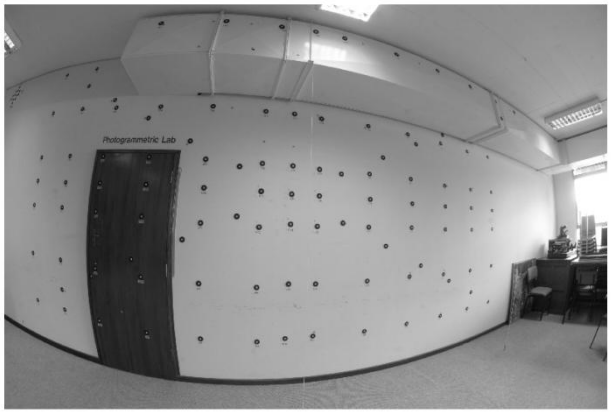

Figure 4a. Original image before image rectification

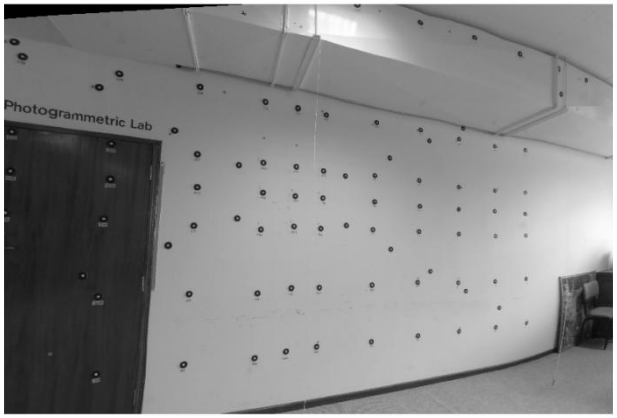

Figure 4b. Rectified image using proposed method

Table 1 shows an extract of five (5) minimum and five (5) maximum displacements of measured image coordinates of control points from their fictitious/ideal image coordinates values (Figure 5). It is observed that the maximum displacements occur at the edges whilst the minimum displacements occur at the central parts of the image. The maximum and minimum displacements are 1344.1 (Point 113) and 1.6 (Point 509) pixels respectively.

Table 1. Extract of ten (10) minimum and maximum image coordinate displacements

	Fictitious Image Coordinates		**Measured Image Coordinates**		**Residuals**		**Displacement**
ID	**x (pixels)**	**y (pixels)**	**x (pixels)**	**y (pixels)**	**x (pixels)**	**y (pixels)**	**(pixels)**
509	2263.0	1435.4	2262.8	1433.9	0.3	1.5	1.6
409	2267.4	1229.9	2266.9	1232.7	0.5	-2.8	2.9
9	1868.9	1452.5	1875.8	1452.3	-6.9	0.2	6.9
6	1873.4	1245.5	1880.4	1246.6	-7.0	-1.0	7.1
3	1866.0	1060.4	1873.7	1064.9	-7.7	-4.4	8.9
601	-435.0	1879.0	395.0	1680.5	-830.0	198.6	853.4
101	-401.9	356.6	455.0	704.2	-856.8	-347.6	924.6
701	-431.6	2275.3	436.2	1922.4	-867.8	352.9	936.8
112	4020.6	-210.5	3234.3	367.7	786.3	-578.2	976.0
113	4566.5	-248.0	3411.3	439.2	1155.1	-687.2	1344.1

An obvious check on the effectiveness of the proposed technique is to verify that a straight line in object space appears as straight line on the image after rectification. This was tested using straight line features in object space and measuring image point coordinates along these lines in the rectified image. The standard deviations of the least squares fit before and after rectification, were used as indicators of line straightness and as a measure of the success of the rectification process.

Table 2. Displacement of interpolated control point from their measured values

ID	Control Point (Measured Value)		Control Point (Interpolated Value)		Residuals		Displacement (pixels)
	x (pixels)	y (pixels)	x (pixels)	y (pixels)	dx (pixels)	dy (pixels)	
5	1680.4	1250.2	1681.4	1251.7	-1.0	-1.5	1.8
304	673.5	1082.2	684.2	1087.1	-10.6	-4.9	11.7
312	3468.6	1006.3	3455.8	1012.0	12.8	-5.7	14.0
610	2713.9	1824.8	2678.1	1815.3	35.7	9.5	37.0
704	692.0	2288.9	694.8	2289.4	-2.8	-0.4	2.8

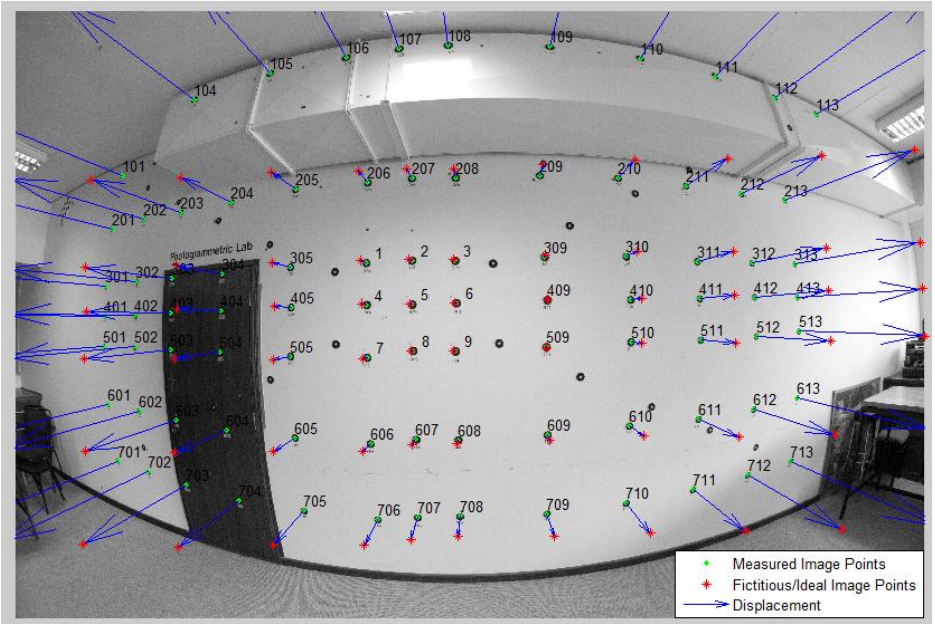

Figure 5. Measured and fictitious image coordinates on original image

For example the standard deviation from seven (7) points along a straight line feature in Figure 6 before (180.6µm equivalent to 28 pixels) and after (17.5µm or approximately 3 pixels) rectification indicate that the effect of lens distortion was successfully minimised using the proposed method.

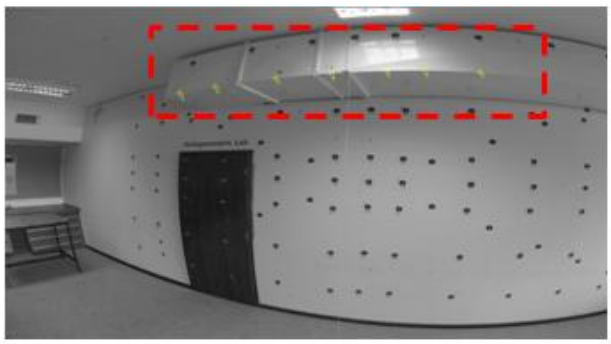

Figure 6a. Measured points (in yellow) on a straight line feature before image rectification

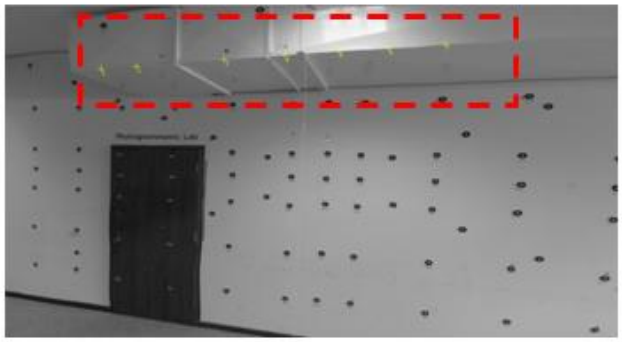

Figure 6b. Measured points (in yellow) on a straight line feature after image rectification

A further numerical test of the proposed method used a subset of the control points to form the image rectification distortion matrix (86 out of 91). The known locations of the five (5) remaining randomly selected control points were compared with their interpolated values. From Table 2 and Figure 7, it is observed that Control points 610 and 5 recorded the maximum and minimum displacements respectively. The denser the control points the more precise the interpolated value. This is an indication that the proposed method is dependent on the distribution and density of control points.

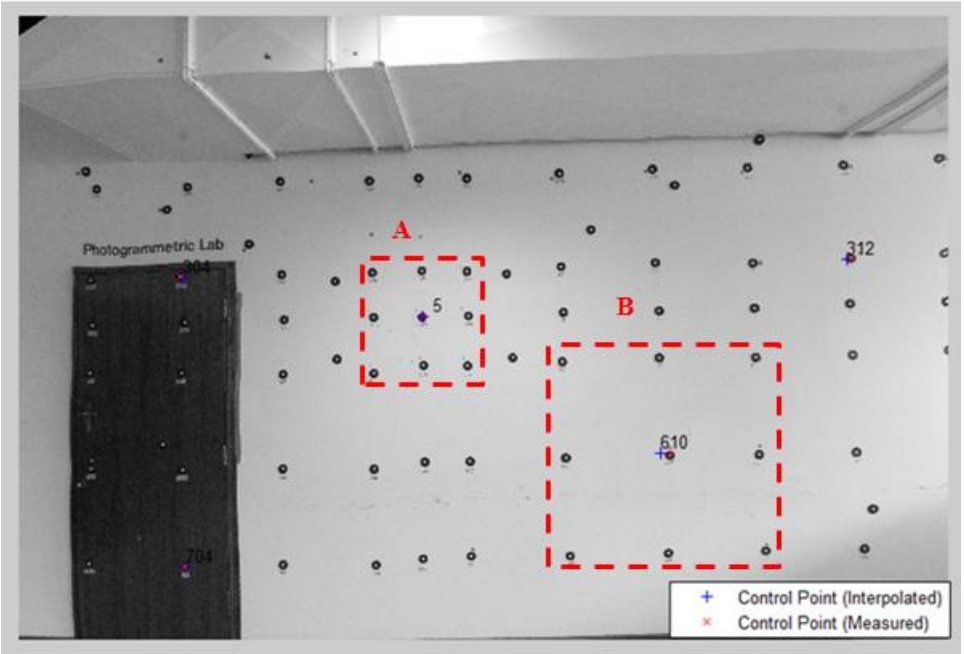

Figure 7. Effect of control points distribution on interpolation

6. Conclusions

The proposed method offers an alternative to the mathematical modelling of lens distortion. First results of the method are encouraging and further tests with a wide range of focal lengths are in progress. It is recommended that for higher accuracy, a dense and well distributed set of control points should be adopted.

The original objective of this research was to develop a method which could be applied to relatively low and medium accuracy photogrammetric object measurements from panorama photography acquired with fisheye lenses. The results now indicate that higher accuracy rectification of panoramic images can be achieved with the proposed method which makes it applicable for wider range of applications.

7. Acknowledgment

This work is supported by the Schlumberger Foundation under the Faculty for the Future

program. The project is carried out as part of a PhD project of the first author and integrated into the Zamani Project initiated and led by Prof Heinz Rüther. The authors are also grateful to the Geomatics Division for making the Division's facilities available for this research.

8. References

Arfaoui A &Thibault S 2013, *'Fisheye lens calibration using virtual grid'*, Applied Optics, vol. 52, no. 12, pp. 2577-2583.

Basu A & Licardie S 1995, *'Alternative models for fish-eye lenses'*, Pattern Recognition Letters, vol. 16, no. 4, pp. 433–441.

Brown DC 1956, *'The simultaneous determination of the orientation and lens distortion of a photogrammetric camera'*, Air Force Missile Test Center Report No. 58-8. Florida: Patrick AFB.

Brown DC 1966, *'Decentering Distortion of Lenses'*, Photometric Engineering, vol. 32, no. 3, pp. 444-462

Brown DC 1971, *'Close-Range Camera Calibration'*, Photogrammetric Engineering, vol. 37, no. 8, pp. 855-866.

Brown DC 1976, *'The bundle adjustment - progress and prospects'*, International Archives of Photogrammetry, vol. 21, no. 3, pp. 33.

Brown DC, Davis RG & Johnson FG 1964, *'The Practical and Rigorous Adjustment of Large Photogrammetric Nets'*, RADC TDR-64-092, Rome Air Development Center, Rome, New York

Clarke TA & Fryer JG 1998, *'The development of camera calibration methods and models'*, The Photogrammetric Record, vol. 16, no. 91, pp. 51-66.

Cronk S, Fraser CS & Hanley H 2006, *'Automatic metric calibration of colour digital cameras'*, The Photogrammetric Record, vol. 21, no.116, pp. 355-372.

Fangi G & Nardinocch C 2013, *'Photogrammetric Processing of Spherical Panoramas',* The Photogrammetric Record, vol. 28, no. 143, pp. 293–311.

Fangi G 2007, *'The Multi-image spherical panoramas as a tool for Architectural Survey'*, XXI International CIPA Symposium, 1-6 October 2007, Atene, CIPA Archives vol. XXI, ISSN 0256-1840, pp. 311-316.

Fangi G 2010, *'Multiscale Multiresolution Spherical Photogrammetry With Long Focal Lenses For Architectural Surveys'*, ISPRS mid-term symposium Newcastle, June 2010

Fraser C 2013, *'Automatic Camera Calibration in Close Range Photogrammetry'*, Photogrammetric Engineering & Remote Sensing, vol. 79, no. 4, pp. 381-388

Fraser CS 1982, *'On the use of non-metric cameras in analytical non-metric photogrammetry'*, International Archives of Photogrammetry and Remote Sensing, vol. 24, no. 5, pp. 156-166.

Fraser CS 1997, *'Digital camera self-calibration'*, ISPRS Journal of Photogrammetry and Remote Sensing, vol. 52, no. 4, pp. 149-159.

Fraser CS, Shortis MR & Ganci G 1995, *'Multi-sensor system self-calibration'*, Videometrics IV, SPIE Proceedings, vol. 2598, pp. 2-18.

Hughes C, Denny P, Jones E & Glavin M 2010, 'Accuracy of fish-eye lens models' Applied Optics, vol. 49, pp. 3338-3347.

Kannala J & Brandt SS 2004, *'A generic camera calibration method for fish-eye lenses'*,17th International Conference on Pattern Recognition (ICPR 2004), Surry, UK, vol. 1, (23-26 August, 2004), pp.10-13.

Kannala J & Brandt SS 2006, *'A generic camera model and calibration method for conventional, wide-angle, and fish-eye lenses'*, IEEE Trans Pattern Anal Mach Intell., vol. 28, no. 8, pp.1335-40

Kedzierski M & Fryskowska A 2008, *'Precise method of fisheye lens calibration'*, International Archives of the Photogrammetry, Remote Sensing and Spatial Information Sciences, vol. XXXVII, pp. 765-768.

Magill AA 1955, *'Variation in distortion with magnification'*, Journal of Research of the National Bureau of

Standards, vol. 54, no. 3, pp.135-142.

Robinson GS 1963, *'The Reseau As a means of detecting gross lack of flatness at the instance of exposure'*, The Photogrammetric Record, vol. 4, no. 22, pp. 283-286.

Rüther H1982, *'Relative Orientation with Limited Control in Close Range Photogrammetry'*, PhD Thesis, University of Cape Town, pp 323.

Rüther H 2002, *'An African Heritage Database: The Virtual Preservation of Africa's Past'*, International Archives of Photogrammetry, Remote Sensing and Spatial Information Sciences, vol. XXXIV, Part 6/W6.

Rüther H 2011, *'Creating Historical Awareness in Africa'*, GIM International, vol. 25, no. 9, http://www.gim-international.com/issues/articles/id1766-Creating_Historical_Awareness_in_Africa.html, date accessed 12/01/2014.

Rüther H, Held C, Bhurtha R, Schroeder, R &Wessels S, 2012, *'From Point Cloud to Textured Model, the Zamani Laser Scanning Pipeline in Heritage Documentation'* South African Journal of Geomatics, vol. 1, no. 1, pp. 44-59.

Sadler LE 1958, *'The significance of Reseau Photography in Triangulation Operations'*, Photogrammetric Engineering, vol. 24, no.1, pp. 132-135.

Schmid HH 1956, *'An Analytical Treatment of the Problem of Triangulation by Stereo-photogrammetry'*, Photogrammetria', vol. 13, no. 2, pp. 67-77 and vol. 13, no. 3, pp. 91-116.

Schneider D, Schwalbe E & Maas HG 2009, *'Validation of geometric models for fisheye lenses'*, ISPRS Journal of Photogrammetry and Remote Sensing, vol. 64, no. 3, pp. 259-266.

Ziemann H 1968, *'Reseau Photography in Photogrammetry - A Review'*, AP- PR-, 39, NRC of Canada, 104081 Ottawa.